Article

a special issue for the scientific conference held by the Department of Chemistry- College of Education for Girls/University of Kufa and in cooperation with Hilla University College, under the title (**5'th Postgraduate Students Annual Conference**) **(PSAC2024)**, which held for Wednesday, **24/4/2024.**

Theoretical study of folic acid and derivatives conjugated with Thymine through Density functional theory

Ayat Ahmed shukrain and Lekaa Hussein Khadim*

*** Department of Chemistry, College of Education for Woman, University of Kufa, Iraq**

liqaa.aljailawi@uokufa.edu.iq

Abstract

The Geometry optimized has been investigated at ground state, B3LYP, 6-311G basis sets with density functional theory (DFT). Theoretical characteristics, like as shape and the HOMO-LUMO gap determined by DFT simulations, help the discovery of donating sites. Global reactivity characteristics of folic acid at the B3LYP/6-311G level have been computed in this work. The global reactivity descriptors include global softness (S), global hardness (η), global affinity (A), ionization potential (I), electro negativity (χ), chemical potential (μ), global electrophilicity index (ω), and global hardness (η). Theoretical spectrograms for the UV and IR spectrum were also constructed at B3LYP values.

Research aims

The main objectives of this work are to provide advice on new derivatives of folic acid, which was done as follows:

1- Diagnosing the effect of structural properties on folic acid derivatives

2- Study the effect of new substituted functional groups on the chemical structure and activity of the drug.

4- Preparing new derivatives and proposed molecular models of the drug as proposed new drugs.

5- Conduct a comparison of the chemical activity, reactivity, and global index parameters of the new proposed optimal model derivative structures with the original folic acid drug.

Keywords: B3LYP, HOMO level, LUMO level, DFT, Folic acid.

Introduction

The B family of vitamins includes thiamine and the folates. Both are converted to active forms that build up in cells and support important metabolic processes. These active forms are not good substrates for export. At physiological pH, thiamine has a positive charge and folates a negative charge (Fig. 1A). Each is delivered to cells by a distinct solute carrier having a high level of structural particularity from the SLC19 family. Thiamine is transported Thiamine transporters 1-ThTr1 and 2-ThTr2, represented by SLC19A2 and SLC19A3,, however folates are not transported via the reduced folate carrier SLC19A1 (RFC). These transporters are the main means by which thiamine and folates are delivered to systemic tissues, and their optimal function is at physiological The intestinal absorption of folates is mediated by pH proton-coupled folate transporter (PCFT), a member of the solute carrier family SLC46A1. Additionally, PCFT is required for folate to pass the blood-brain barrier, choroid plexus, and cerebrospinal fluid barrier. Two folate membrane receptors, FOLR1 and FOLR2, mediate an endocytic process that transports folates as well. SLC46A1 is not classified in the Saier "transporter classification system" (http://www.tcdp.org/), although SLC19A1-3 belongs to the 2A.48 subfamilies. The loss-of-function mutations in SLC19A2, SLC46A1, FOLR1, and, to a lesser extent, SLC19A2 have resulted in autosomal recessive hereditary illnesses that have defined their physiological roles. In order to treat cancer and inflammatory/autoimmune illnesses, respectively, folate transporters are crucial in delivering analogues of folate in inflammatory and cancerous cells. A unique method for the targeted delivery of medications to malignant and immunological cells is the development of folic acid-based diagnostic and therapeutic compounds that are incorporated into the cells through a process called folate receptor mediated endocytosis. A significant portion of our

knowledge regarding the mechanisms behind folate transport comes from research conducted on folate analogues, such as pemetrexed and, more recently, methotrexate. [1], [2], [3]

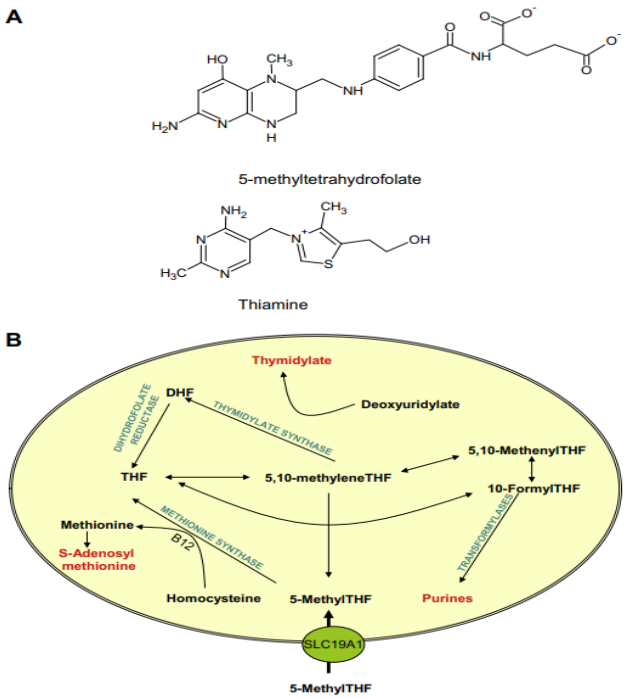

Figure (1): (A) Thiamine and 5-MTHF structures ,(B) Metabolic reactions for homocysteine and 5-methylTHF, methionine synthesis, THF production, one-carbon derivatives for purine and thymidylate synthesis, DHFR inhibition by methotrexate and pralatrexate, Pemetrexed's derivatives for purine ring synthesis, and direct inhibitors of thymidylate synthase.[4]

Computational methods

We drew the folic acid complex using the Gauss View program 06 and used Gaussian 09 [5][6] to calculate it using DFT / B3LYP in the basis set 6-311G[7], where the engineering optimization structure were built. In addition to calculating the energy of the folic acid as a whole, the energy of the transition between the lowest electron-occupied orbit (LUMO) and the highest electron-occupied orbit (HOMO), and the energy difference between the orbits[8] In theoretical chemistry, the chemical potential (μ) is defined as the electronegativity's negative (χ). [9] as:

$$\chi = \frac{1}{2}\,(\boldsymbol{E\ Lumo} + \boldsymbol{E\ Homo}) \quad \ldots\ldots\ldots\ldots\ldots \mathbf{1}$$

$$\mu = -\chi = \frac{1}{2}\ (\boldsymbol{E\ Lumo + E\ Homo}\ ) \ldots\ldots\ldots\ldots \mathbf{2}$$

The hardness (η) quantitative description With a total energy power of E, an N-electron device can be expressed as [10]

$$\eta = \frac{1}{2}\ (\boldsymbol{E\ Lumo - E\ Homo}\ ) \ldots\ldots\ldots\ldots\ldots \mathbf{3}$$

The worldwide electrophilicity index (ω) [11] In terms of is conveyed as:

$\omega = -\frac{\mu 2}{2\,\eta}$ …… 4

where the chemical system's initial potential for vertical ionization and electron affinities are, respectively, IP and EA. Koopmans' theorem can be used to express the aforementioned parameters as an additional approximation. [12].

I = - E Homo …….. 4

A= - E Lumo ……... 5

where the lowest unoccupied molecular orbital's energy is known as ELUMO and the highest occupied molecular orbital's energy is known as EHOMO. Moreover, the visible UV spectrum was calculated to determine the maximal wavelength of the folic acid complex, and the infrared spectrum was used to diagnose the condition.

Results and Discussion

Geometry optimization of Folic acid

Folic acid's optimally structured shapes Fig. 2, DFT /B3LYP /6-311G, covers all of the useful conclusions from the present investigation.

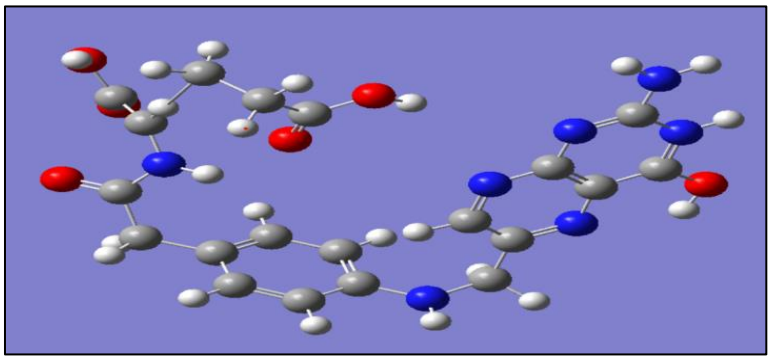

. Fig. 2 Geometry optimized for Folic acid by DFT/ B3LYP basis set 6-311G .

Properties of Folic acid

Molecular Electrostatic Potential

Studying the electrostatic potential of the molecule gives us a clear picture of the electronic density distribution of molecular systems to predict and verify chemically active sites with high electronegativity with a center of positive charge by drawing the peripheral surface (2D) of the molecules [13] .

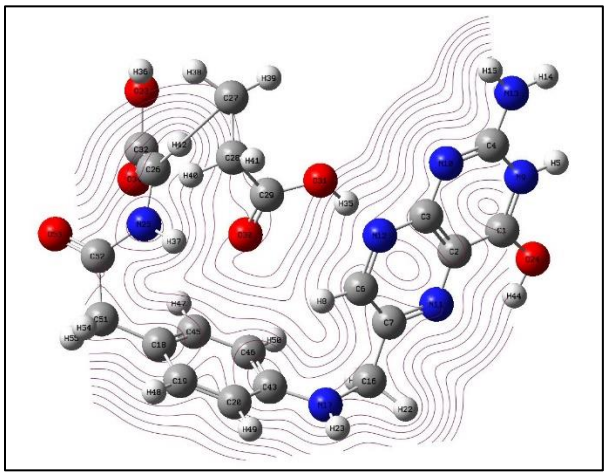

Fig.3 Total density of 2D for Folic acid by DFT/ B3LYP basis set 6-311G

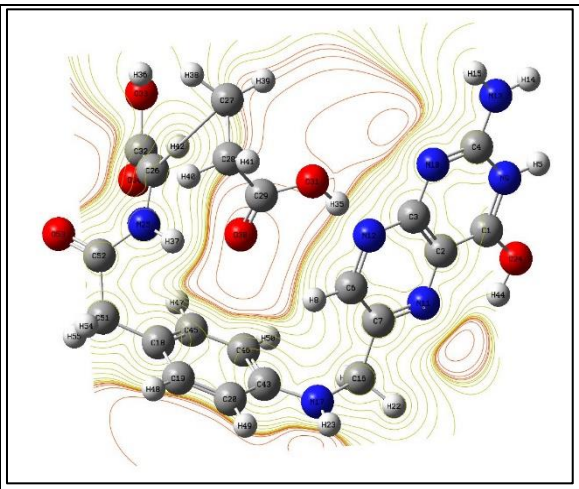

Fig.4 ESP of 2D for Folic acid by DFT/ B3LYP basis set 6-311G .

Energy levels

The DFT using B3LYP/6-311G was used to calculate the energy of folic acid's frontal molecular orbitals, including EHOMO, ELUMO, and Egap. Whereas the energy of ELUMO is associated with the potential to take electrons from the molecules, the energy of the electron-donating potential of EHOMO is commonly related to the molecules. [14]. Both the LUMO value and the high-value EHOMO indicate a strong tendency to accept electrons and a heavy inclination to give electrons with low empty molecular orbital energy to a suitable acceptor molecule. Table 1 and Figure 5 present the results, which indicate which form of folic acid has the highest LUMO energy. The disparity in energy between folic acid's HOMO and LUMO energy levels [15]. Low electronic stability and high reactivity arise from low energy gap values. Low values can be advantageous since they indicate that it would be simple to extract an electron from the HOMO orbital and transfer

it to the LUMO orbital. lead to reaction The formula (1) Hartree = (27.211 e.v) converts the energy units of the Hartree to electron volts.

Table 1 . Levels of energy in folic acid at DFT/6-311G at levels of theory.

Functions	E_{LUMO}	E_{HOMO}	ΔE gap
Folic acid	-0.09404	-0.17731	0.08327

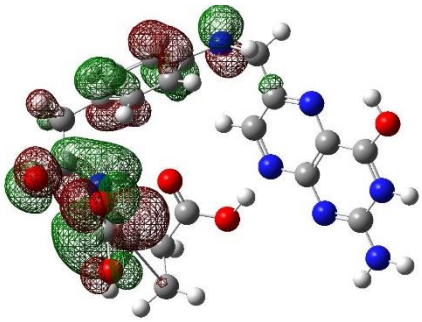

EHOMO=-0.1773

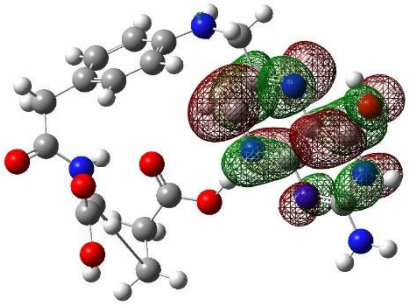

Egap=0.0832

ELUMO=-0.0940

Fig.5. The DFT/B3LYP basis set 6-311G provides the energy of the LUMO and HOMO molecular orbitals of folic acid.

Global Reactivity Descriptors

Determine the values of the following: ionization potential (I), global hardness (η), chemical potential (μ), electronegativity (χ), global electrophilicity index (ω), and electronic affinity (A) in table (2). [16], According to the results, a low stable structure is indicated by a low hardness value, while a tiny ionization potential value suggests a high level of reactivity of the atoms and molecules. The electrophilic energy calculation of a gain the electrophilicity (ω) toward a

nucleophile in the molecular process. A molecule's reactivity as an electrophile increases with its electrophilic ability. The design shows low hardness and a strong reactivity, as indicated by its electrophilic value. [17].

Table 2. Folic acid properties via DFT/B3LYP/6-311G

Folic acid	μ (eV)	X (eV)	ω (eV)	η (eV)	I (eV)	A (eV)
	-0.1356	0.1356	-0.221	0.0416	0.1773	0.0940

Spectroscopy properties

1-UV-Visible spectrophotometer

Fig.6 demonstrates an absorption peak measured by UV-visible spectroscopy at the maximum wavelength of 658 nm. This helps us to explain why the produced complex has color because the visible range, which spans 450–960 nm, is covered by this wavelength.

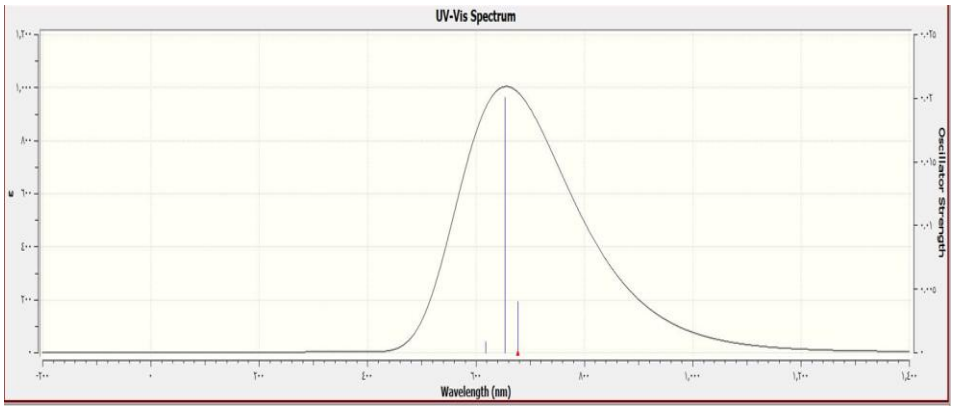

Fig. 6. UV- visible spectroscopy of folic acid by DFT/ B3LYP basis set 6-311G .

2-Infrared spectroscopy

The folic acid's ground state harmonic vibrational frequencies, B3LYP, and 6-311G base sets displayed in Fig. 7 were investigated. There were two sorts of stretching anomalies, including symmetric ones, in addition to asymmetric varieties. While the asymmetric stretching occurred in distinct periods while the bonds vibrated, the symmetric stretching occurred within the same period as the atoms. Multiple bands of the aliphatic (C-H) There are stretching vibrations seen in the vicinity of 1500 cm-1.[18]. At 1200 cm-1, 1250 cm-1, 1850 cm-1, and 3442

cm-1, a new band emerges. Specifically, the υ (C-C), υ (C-N), υ (C=O), and υ (N-H). Using the Gussain09 program, theoretical vibrational decomposition calculations of folic acid were performed. [19].

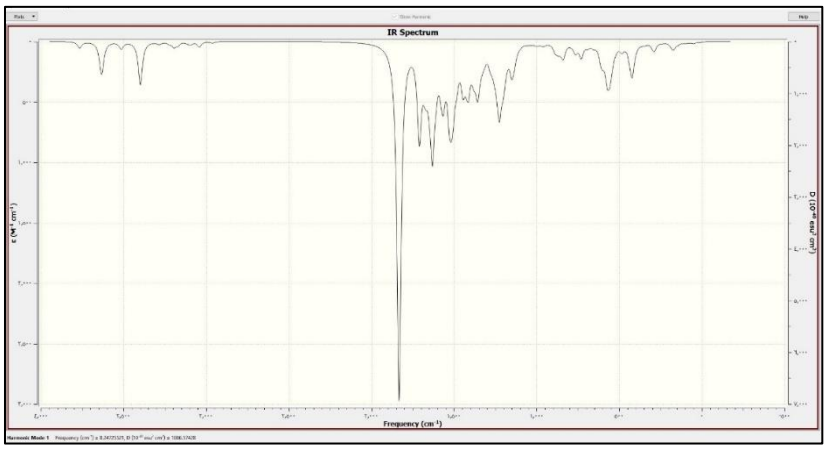

Fig. 7. Folic acid infrared spectroscopy using DFT/B3LYP basis set 6-113G.

Binding with thymidine in DNA

The metabolism of folic acid produces building components of nucleic acids, which are essential for DNA creation and maintenance. Deoxyuridine monophosphate (dUMP) gains a methyl group from thymidylate synthase., which initiates the de novo production of deoxythymidine monophosphate (dTMP). After that, this substance undergoes phosphorylation to produce thymidine triphosphate (dTTP) and deoxynucleotide triphosphate (dNTP). Thymidine triphosphate (dTTP) is one of the four deoxyribonucleic acids involved in DNA synthesis and repair. A lack of folate will prevent the conversion of deoxyuridine triphosphate (dUMP) to dTMP, resulting in an excess of dUTP. [20] . The binding of Original folic acid and folic acid_O54-CH3 to thymine at various locations depicted in Figure 7 was calculated theoretically. We favor the bond of folic acid_O_{54}-CH_3 over the original folic acid because, according to the binding energy calculation, the binding energy of thymine in folic acid_O54-CH3 is lower than the binding energy of the original folic acid. The folic acid O54-CH3 has a greater Egap and chemical hardness (η), indicating a more stable structural structure than the original folic acid binding, and a lower electrophilicity (Þ) indicating less reactive activity. When compared to Original Folic acid binding, Folic acid _O_{54}-CH_3 exhibits more DNA distortion efficacy. The Folic acid _O54-CH3 is more successful in bending the DNA strand when it binds to the DNA strand because it is more stable and inhibits DNA

resistance to it when it binds from Original Folic acid binding. Table displays the outcomes (3).

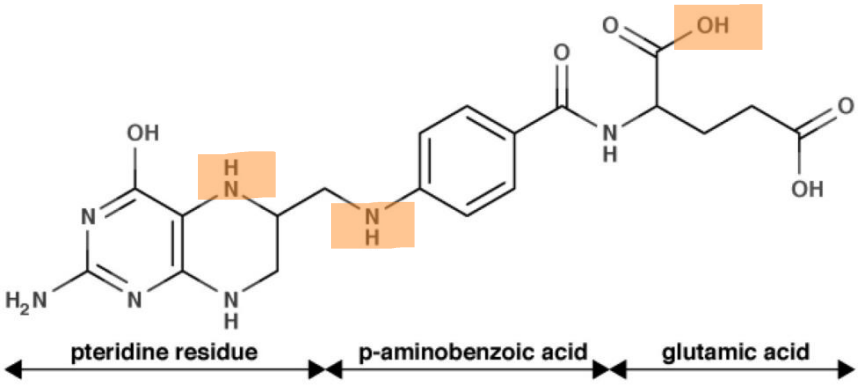

Figure8: shows the binding sites of folic acid to thymine

Table 3. Mathematical comparison between original folic acid and Folic acid _O_{54}-CH_3 using a distribution of Semi/B3LYP/6-311G

Complex type	μ	E gap	η	ω
original folic acid	-0.1933 e.v	0.2511e.v	0.1255 e.v	-0.1487 e.v
Folic acid _O_{54}-CH_3	-1.249 e.v	0.2242e.v	0.1440e.v	-5.419 e.v

The measured geometric parameters of the compound $O_{54}CH_3$-folic acid were also obtained before binding to thymine, and the geometric parameters were measured and compared after binding to thymine.

As shown in Table (4). From table (3) as shown the bond length for Folic acid $O_{54}CH_3$ + Thymine is lower value .

Table 4. Calculate the length of the bond using DFT/B3LYP/6-311G of folic acid, both theoretically and empirically.

Folic acid $O_{54}CH_3$		**Folic acid O54CH3 + Thymine**	
Bond length	Bond angle	Bond length	Bond angle
1.248 A^0	119.985	1.88 A^0	119.211

References

[1] L. H. Matherly, M. R. Wilson, and Z. Hou, "The major facilitative folate transporters solute carrier 19A1 and solute carrier 46A1: biology and role in antifolate chemotherapy of cancer," *Drug Metab. Dispos.*, vol. 42, no. 4, pp. 632–649, 2014.

[2] R. Zhao, N. Diop-Bove, M. Visentin, and I. D. Goldman, "Mechanisms of membrane transport of folates into cells and across epithelia," *Annu. Rev. Nutr.*, vol. 31, pp. 177–201, 2011.

[3] M. Visentin, N. Diop-Bove, R. Zhao, and I. D. Goldman, "The intestinal absorption of folates," *Annu. Rev. Physiol.*, vol. 76, pp. 251–274, 2014.

[4] M. Bevensee, *Co-transport systems*, vol. 70. Academic Press, 2012.

[5] M. J. Frisch *et al.*, "09, Revision D. 01, Gaussian," *Inc., Wallingford, CT*, 2009.

[6] B. Szefler, P. Czeleń, S. Kruszewski, A. Siomek-Górecka, and P. Krawczyk, "The assessment of physicochemical properties of Cisplatin complexes with purines and vitamins B group," *J. Mol. Graph. Model.*, vol. 113, p. 108144, 2022.

[7] A. Noori Tahneh, S. Bagheri Novir, and E. Balali, "Density functional theory study of structural and electronic properties of trans and cis structures of thiothixene as a nano-drug," *J. Mol. Model.*, vol. 23, pp. 1–15, 2017.

[8] D. Veclani, A. Melchior, M. Tolazzi, and J. P. Cerón-Carrasco, "Using theory to reinterpret the kinetics of monofunctional platinum anticancer drugs: stacking matters," *J. Am. Chem. Soc.*, vol. 140, no. 43, pp. 14024–14027, 2018.

[9] H. Tandon, T. Chakraborty, and V. Suhag, "A scale of atomic electronegativity in terms of atomic nucleophilicity index," *Found. Chem.*, vol. 22, pp. 335–346, 2020.

[10] M. BOUACHRINE *et al.*, "DFT/TDDFT studies of the structural, electronic, NBO and non-linear optical proper-ties of triphenylamine functionalized tetrathiafulvalene," *Turkish Comput. Theor. Chem.*, vol. 5, no. 2, pp. 24–34, 2021.

[11] L. von Szentpály, S. Kaya, and N. Karakuş, "Why and when is electrophilicity minimized? New theorems and guiding rules," *J. Phys. Chem. A*, vol. 124, no. 51, pp. 10897–10908, 2020.

[12] J. E. Turner, V. E. Anderson, and K. Fox, "Ground-state energy eigenvalues and eigenfunctions for an electron in an electric-dipole field," *Phys. Rev.*, vol. 174, no. 1, p. 81, 1968.

[13] K. D. Dobbs and W. J. Hehre, "Molecular orbital theory of the properties of inorganic and organometallic compounds. 6. Extended basis sets for second-row transition metals," *J. Comput. Chem.*, vol. 8, no. 6, pp. 880–893, 1987.

[14] A. Parandaman and B. Rajakumar, "Addition and abstraction kinetics of H atom with propylene and isobutylene between 200 and 2500 K: A DFT study," *Chem. Phys.*, vol. 491, pp. 82–94, 2017.

[15] M. Sahadevan, M. Sundaram, and K. Subramanian, "Quantum mechanical approaches and molecular docking studies of metal based anticancer drugs cis-Diammine glycolato platinum and Diaminocyclohexane oxalatoplatinum structures," *Comput. Biol. Chem.*, vol. 106, p. 107940, 2023.

[16] R. Xia *et al.*, "Stable isotope ratios trace the rice uptake of cadmium from atmospheric deposition via leaves and roots," *Environ. Sci. Technol.*, vol. 57, no. 44, pp. 16873–16883, 2023.

[17] S. Kaya and M. V Putz, "Atoms-In-Molecules' Faces of Chemical Hardness by Conceptual Density Functional Theory," *Molecules*, vol. 27, no. 24, p. 8825, 2022.

[18] L. Li, T. Cai, Z. Wang, Z. Zhou, Y. Geng, and T. Sun, "Study on molecular structure, spectroscopic investigation (IR, Raman and NMR), vibrational assignments and HOMO–LUMO analysis of L-sodium folinate using DFT: A combined experimental and quantum chemical approach," *Spectrochim. Acta Part A Mol. Biomol. Spectrosc.*, vol. 120, pp. 106–118, 2014.

[19] M. A. Palafox, V. K. Rastogi, and S. P. Singh, "FT-IR and FT-Raman spectra of 5-chlorocytosine: Solid state simulation and tautomerism. Effect of the chlorine substitution in the Watson-Crick base pair 5-chlorodeoxycytidine-deoxyguanosine," *Spectrochim. Acta Part A Mol. Biomol. Spectrosc.*, vol. 188, pp. 418–435, 2018.

[20] S. J. Duthie, "Folate and cancer: how DNA damage, repair and methylation impact on colon carcinogenesis," *J. Inherit. Metab. Dis.*, vol. 34, pp. 101–109, 2011.